The quasi-unchanged gas-phase molecular structures of the atmospheric aerosol precursor β-pinene and its oxidation product nopinone

E. Neeman, J.-R. Avilés-Moreno, T. Huet

Journal Name

ARTICLE

The quasi-unchanged gas-phase molecular structures of the atmospheric aerosol precursor β-pinene and its oxidation product nopinone

Received 00th January 20xx,
Accepted 00th January 20xx

DOI: 10.1039/x0xx00000x

www.rsc.org/

E. M. Neeman,[a] J.-R. Avilés-Moreno [a] and T. R. Huet [a,†]

The rotational spectra of the two bicyclic molecules β-pinene and its oxidation product nopinone were investigated in the gas phase, by Fourier transform microwave spectroscopy coupled to a supersonic jet, in the 2-20 GHz range. The parent species and all heavy atom isotopologues have been observed in their natural abundance. The spectroscopic parameters of the ground states were determined from a Watson's Hamiltonian in the A reduction. The rotational constants were used together with geometrical parameters from *ab initio* calculations to determine the r_0 and $r_m^{(1)}$ structures of the skeletons, without any structural assumption in the fit concerning the heavy atoms. Comparison with solid phase and other bicyclic monoterpenes unveiled an unprecedented complete set of geometrical parameters for the rigid cages. The structures of β-pinene and nopinone are very close, except for the substituents at C_2. In the gas phase C_2 is a centre of planarity in both molecules.

Introduction

Monoterpenes are unsaturated $C_{10}H_{16}$ hydrocarbons of primordial atmospheric interest, regarding the production of biogenic volatile organic compounds (BVOCs) emitted by biomasses. Recently a direct pathway was found in laboratory from the oxidation of several BVOCs, such as cyclic monoterpenes, to the formation of large amounts of extremely low-volatility vapours, which condense irreversibly onto aerosol surfaces to produce secondary organic aerosol.[1] β-pinene (6,6-dimethyl-2-methylenebicyclo[3.1.1]heptane, $C_{10}H_{16}$) is a bicyclic monoterpene of atmospheric interest. The β-pinene molecule (Fig. 1) is emitted into the atmosphere by pine forests.[2] It has also been identified as a major monoterpene emitted by several different plants.[3] In addition, it is issued in large quantities in the centre of the Amazon by tropical forest.[4] It is known for its short lifetime (a few hours) into the atmosphere[5,6] and it participates in the formation of the secondary organic aerosols.[7,8] In particular Yu *et al* have studied in details the ozonolysis of four monoterpenes,[9] including α- and β-pinene, and reported the products emitted during this reaction. The major product of the O_3 oxidation of β-pinene is nopinone (6,6-dimethylbicyclo[3.1.1]heptan-2-one, $C_9H_{14}O$). Similar studies on the same reaction also showed that the nopinone molecule (Fig. 1) is a major product.[10,11]

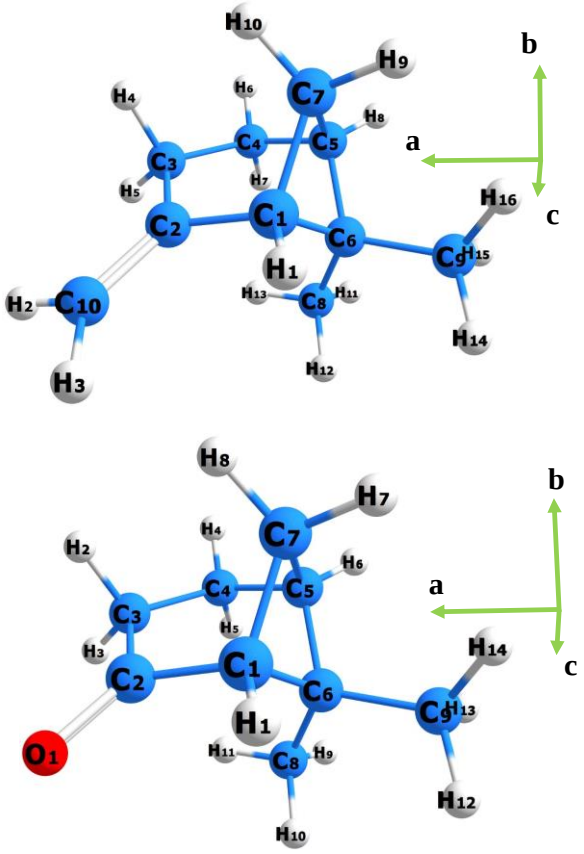

Figure 1 Equilibrium geometry of observed conformer of β-pinene ($C_{10}H_{16}$) (upper) and nopinone ($C_9H_{14}O$) (lower), calculated at the MP2/aug-cc-pVTZ level, and the numbering of all atoms. The principal axis systems are also presented.

[a] *Univ. Lille, CNRS, UMR 8523 - PhLAM - Physique des Lasers Atomes et Molécules, F-59000 Lille, France.*
† Corresponding author: Therese.Huet@univ-lille1.fr, http://orcid.org/0000-0001-9104-5156.
Electronic Supplementary Information (ESI) available: [Fits: Spectroscopy and Structures]. See DOI: 10.1039/x0xx00000x

Other studies have been carried out on the reaction of β-pinene with the OH radical which have shown that nopinone is also one of the major products of this reaction.[12,13] Finally the results from a series of outdoor chamber experiments showed that both the ozonolysis of β-pinene and its reaction with OH produce secondary organic aerosols (SOA).[14,15]

Regarding physical chemistry, the ozone initiated chemistry is generally believed to lead to the formation of Criegee intermediates.[16] Ozonolysis reactions of bicyclic monoterpenes is a current subject of investigation, using quantum chemistry calculations. The first step of the Criegee mechanism is the cycloaddition of ozone to the double bond of these unsaturated species, and it is believed to be rate determining in the complete mechanism. A good knowledge of the structure of these monoterpenes is a pre-requisite to model their kinetics.[16,17] In this study we present the gas-phase structure determination of β-pinene and nopinone, using microwave spectroscopy and quantum chemical calculations. Our aim was to compare the structures of the reagent and of its oxidation product. This point is also of interest in organic chemistry especially for understanding the variation in bond length and angles due to the presence of stress. To the best of our knowledge only solid phase structural information from X-ray diffraction studies of β-pinene and nopinone have been published.[18,19] Both molecules are rigid cages and as such are presenting only one stable conformer. The spectroscopic information available on gas phase $C_{10}H_{16}$ monoterpenes are rather scarce. The microwave spectroscopy of limonene has revealed a monocyclic structure with three equatorial conformers,[20] and the detailed structure of camphene, a bicyclic molecule, was recently obtained by combining experimental spectroscopic parameters to calculated geometries.[21] Concerning monoterpenoids the rotational spectrum of camphor ($C_{10}H_{16}O$), which is one oxidation product of camphene, has been studied in the pioneering work of Kisiel and co-workers by rotational spectroscopy and quantum calculations, allowing the determination of precise structural parameters.[22] More recently the bicyclic structure of fenchone ($C_{10}H_{16}O$) was also characterized.[23] For both molecules it was found necessary to made structural assumptions in order to keep the precision of the fitted parameters. In this work rotational spectroscopy has been used to characterise the structure of β-pinene and nopinone. The impulse Fabry-Pérot Fourier-transform microwave technique coupled to a pulsed molecular beam was used (FP-FTMW spectrometer).[24-26] The sensitivity of the technique allowed the observation of isotopologues in their natural abundance, even if the rotational spectrum is not intense, as observed for β-pinene. The rotational constants of all observed species have been used to determine the substitution (r_s), the ground-state (r_0) and the equilibrium related, mass-dependence ($r_m^{(1)}$) geometries.[27-30] Structures have been compared with those calculated by theoretical methods and with the crystal structures obtained by X-ray diffraction. Finally our results were also compared with those obtained for related terpenoids.

Experimental

The pure rotational (2-20 GHz) spectrum of β-pinene and nopinone were recorded using the Lille MB-FTMW spectrometer.[31-32] β-pinene (96%) and nopinone (98%) were purchased as liquid samples from Sigma-Aldrich and used without any further purification. Both samples were heated in a reservoir in order to be vaporized. The optimum signals of β-pinene and nopinone were obtained at a temperature of 363 K and 343 K, respectively. Neon was used as carrier gas and flowed through the heated nozzle at a stagnation pressure of 4 and 3 bars, respectively. The mixtures were introduced into the Fabry-Pérot cavity along the optical axis, through a 1 mm diameter pinhole by means of a pulsed nozzle at a repetition rate of 1.5 Hz. The rotational temperature (T_{rot}) of the supersonic jet was about a few Kelvin. Microwave power pulses of 2 μs duration were used to polarize the molecules. The Free-Induction Decay (FID) signal was detected and digitized at a repetition rate of 120 MHz. FID signals were accumulated in order to obtain a good S/N ratio. About thirty and a few hundred FID signals were accumulated in the low resolution scan mode and in the high resolution measurement mode, respectively. After a fast Fourier transformation of the time domain signals, lines were observed as Doppler doublets (~10 kHz full width at half maximum, FWHM). The central frequency of each line was determined by averaging the frequencies of the two Doppler components. The spectral resolution is depending on the number of recorded data points, *i. e.* most of the time with a frequency grid of 0.92 or 1.84 kHz. By optimizing the temperature in order to minimize the decomposition of the samples, spectra were left with strong signals associated with the parent molecules, and weak signals associated with ^{13}C and ^{18}O isotopomers. A portion of the rotational spectrum of β-pinene in the low resolution scan mode is shown in Fig. 2a. The high sensibility of our spectrometer with S/N ratios of about 10^5:1 allowed the observation of the ten singly substituted ^{13}C isotopologues in natural abundances (1.109%). The same situation was observed for the ^{13}C isotopomers of nopinone, as illustrated in Fig. 2b. In addition weak signals of the ^{18}O isotopologue (0.205%) were also identified.

Quantum chemical calculations

The quantum chemical calculations were performed using the Gaussian 09, Rev. D.01, software package (G09)[33] and visualized using the Chemcraft program.[34] The structures of β-pinene and nopinone were optimized using *ab initio* calculations at the MP2 level of the theory (Møller-Plesset second order perturbation theory),[35] with the Dunning's correlation consistent triple-zeta aug-cc-pVTZ basis set with added polarization functions[36] in order to obtain an equilibrium structure which could be compared with the experimental structural parameters. The molecular parameters and the harmonic force field have also been evaluated with the Pople split-valence triple-zeta basis set augmented with diffuse and polarization functions on all

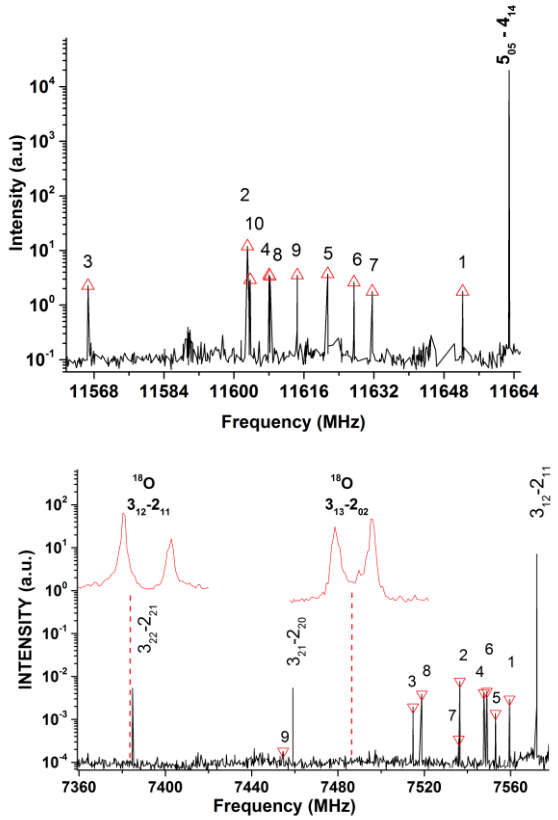

Figure 2 A portion of the spectrum showing the rotational lines $J_{KaKc}=5_{05}-4_{14}$ and $J_{KaKc}=3_{12}-2_{11}$ of β-pinene (upper) and nopinone (lower), respectively. The rotational lines of the ten singly substituted ^{13}C isotopologues are also shown, with the identity of the substituted ^{13}C atom in the molecule (1 to 10). The low resolution scan mode of the FP-FTMW spectrometer was used. Intensity is in arbitrary unit. Insert: signal for the ^{18}O isotopologue of nopinone at high resolution, 1000 accumulations.

atoms (the 6-311++G(d,p) basis set).[37] The principal rotational constants (A, B, C), and the quartic centrifugal distortion parameters (Δ_J, Δ_{JK}, Δ_K, δ_J, δ_K) have been calculated for the main species, as well as the electric dipole moment components. These parameters have also been evaluated using the B3LYP[38-39] and the M06-2X[40-41] density functional with the 6-311++G(2df,p) basis set. There is no splitting of lines due to internal rotation of the two methyl groups attached to the (C_6) carbon atom. These barriers were calculated at about 1000 cm^{-1} and 1380 cm^{-1} for β-pinene and nopinone, respectively.

Results

Molecular parameters

More than hundred observed lines were assigned to a-type, b-type and c-type transitions for both β-pinene and nopinone molecules, up to J=8 and K_a=6. The SPFIT/SPCAT suite of programs developed by Pickett[42] was used to fit the observed transitions to a Watson's Hamiltonian[43] in the A-reduction:

$$H_{rot}^{(A)} = B_x^{(A)}J_x^2 + B_y^{(A)}J_y^2 + B_z^{(A)}J_z^2 - \Delta_J\vec{J}^4 - \Delta_{JK}\vec{J}^2J_z^2 - \Delta_KJ_z^4 - \frac{1}{2}\left[\delta_J\vec{J}^2 + \delta_KJ_z^2, J_+^2 - J_-^2\right]_+$$

and in the I^r representation. The fitted values of the rotational (A, B, C) and centrifugal distortion (δ, Δ) constants along with the root mean square value on the line frequencies (RMS) are presented in Table 1 for the parent species. All the assigned lines of β-pinene and nopinone are available as supplementary material, with the SPFIT output files reformatted with the PIFORM program.[44] Ground state experimental molecular parameters values can be compared to listed theoretically calculated values at equilibrium position.

Both molecules being chiral all carbon atoms are non-equivalent. The spectra of all ^{13}C isotopologues were searched for in order of increasing distance of the substituted carbon from the centre of mass. The ab initio structure evaluated at the MP2/aug-cc-pVTZ level was used to calculate the rotational constants for the singly substituted ^{13}C and ^{18}O isotopologues, with the CORSCL program.[44] The values of the calculated rotational constants were then scaled by the ratio

Table 1 Rotational constants, quartic centrifugal distortion parameters, and dipole moment components of β-pinene and nopinone, determined experimentally from the ground state, and theoretically from the equilibrium structure. The root mean square (RMS) value on the line frequencies and the number of data (N) are also indicated.

β-pinene	Exp.	B3LYP[a,b]	M062X[a,b]	MP2[a,c]	MP2[a,d]
A/MHz	1901.889134(82)	-0.2%	-0.8%	-0.1%	-0.8%
B/MHz	1293.6600842(41)	0.7%	-1.0%	-0.7%	-1.6%
C/MHz	1150.831081(42)	0.5%	-0.9%	-0.3%	-1.2%
Δ_J/kHz	0.07551(39)	5.3%	-0.7%	0.7%	-
Δ_{JK}/kHz	-0.0324(21)	25.6%	-9.2%	-2.5%	-
Δ_K/kHz	0.0761(26)	5.6%	-3.2%	2.0%	-
δ_J/kHz	0.01876(22)	8.4%	-4.1%	0.2%	-
δ_K/kHz	-0.0503(32)	-2.4%	2.8%	28.4%	-
RMS/kHz	1.23	-	-	-	-
N	119	-	-	-	-
$\lvert\mu_a\rvert$/D	-	0.43	0.42	0.49	0.50
$\lvert\mu_b\rvert$/D	-	0.58	0.56	0.62	0.63
$\lvert\mu_c\rvert$/D	-	0.11	0.12	0.14	0.13
Nopinone	Exp.	B3LYP[a,b]	M062X[a,b]	MP2[a,c]	MP2[a,d]
A/MHz	1923.079394(124)	-0.2%	-0.7%	0.02%	-0.5%
B/MHz	1297.571854(78)	1.0%	-1.1%	-0.8%	-1.9%
C/MHz	1164.017499(85)	0.6%	-1.0%	-0.3%	-1.2%
Δ_J/kHz	0.10346(79)	5.2%	1.8%	2.6%	-
Δ_{JK}/kHz	-0.0942(37)	35.0%	13.8%	22.1%	-
Δ_K/kHz	0.1311(56)	30.9%	22.4%	29.7%	-
δ_J/kHz	0.03110(47)	8.3%	2.3%	4.8%	-
δ_K/kHz	-0.0324(110)	-49.7%	50.0%	55.6%	-
RMS/kHz	1.86	-	-	-	-
N	119	-	-	-	-
$\lvert\mu_a\rvert$/D	-	2.25	2.18	2.47	2.44
$\lvert\mu_b\rvert$/D	-	2.64	2.64	3.06	3.01
$\lvert\mu_c\rvert$/D	-	0.32	0.35	0.38	0.40

[a] Deviation (%) calculated as (Exp-Theo)/Exp ; [b] 6-311++G(2df,p) basis set ; [c] 6-311++G(d,p) basis set ; [d] aug-cc-pVTZ basis set.

Table 2 Rotational constants and quartic centrifugal distortion parameters for the ^{13}C and ^{18}O isotopologues of β-pinene and nopinone, determined experimentally from the ground state. The root mean square (RMS) value on the line frequencies and the number of fitted lines (N) are also indicated. The values of the quartic centrifugal distortion constants (Δ_K, Δ_{JK}, δ_J, and δ_k for β-pinene and δ_k for nopinone) were kept fixed to those obtained for the parent species.

β-pinene	**$^{13}C_1$**	**$^{13}C_2$**	**$^{13}C_3$**	**$^{13}C_4$**	**$^{13}C_5$**
A/MHz	1894.0328(14)	1899.8107(10)	1895.8035(13)	1878.2029(42)	1891.7105(11)
B/MHz	1291.12357(41)	1287.27072(27)	1283.72456(38)	1291.1367(11)	1291.59469(33)
C/MHz	1150.04857(20)	1145.30340(11)	1141.54329(20)	1143.14149(49)	1145.46166(15)
Δ_J/kHz	0.0756(19)	0.07780(84)	0.0755(20)	0.0665(40)	0.0779(13)
N	13	12	12	14	16
RMS/kHz	0.6	0.2	0.5	1.1	0.5
	$^{13}C_6$	**$^{13}C_7$**	**$^{13}C_8$**	**$^{13}C_9$**	**$^{13}C_{10}$**
A/MHz	1900.9961(15)	1881.7682(45)	1878.4290(25)	1897.8335(20)	1885.8091(32)
B/MHz	1289.75731(41)	1286.3789(12)	1283.15066(69)	1273.53678(55)	1276.99920(78)
C/MHz	1147.59339(20)	1148.60619(67)	1146.60842(35)	1133.86192(27)	1132.08127(37)
Δ_J/kHz	0.0710(19)	0.0724(70)	0.0719(33)	0.0777(26)	0.0805(30)
N	14	12	14	13	13
RMS/kHz	0.6	0.6	1.0	0.8	0.8
Nopinone	**$^{13}C_1$**	**$^{13}C_2$**	**$^{13}C_3$**	**$^{13}C_4$**	**$^{13}C_5$**
A/MHz	1914.89569(23)	1920.96273(46)	1916.68508(31)	1898.37181(21)	1912.52742(21)
B/MHz	1294.993562(96)	1291.42523(17)	1287.81886(16)	1295.23573(13)	1295.39145(14)
C/MHz	1163.189369(78)	1158.55460(13)	1154.91052(12)	1155.910888(85)	1158.396672(98)
Δ_J/kHz	0.09900(91)	0.1015(16)	0.0963(14)	0.1000(12)	0.0999(13)
Δ_{JK}/kHz	-0.0882(57)	-0.0907(62)	-0.0656(78)	-0.0991(55)	-0.0841(56)
Δ_K/kHz	0.163(19)	0.143(37)	0.155(22)	0.105(11)	0.150(11)
δ_J/kHz	0.02902(73)	0.0308(13)	0.0260(12)	0.02855(89)	0.03104(97)
N	35	42	43	42	39
RMS/kHz	0.65	1.23	1.27	1.06	1.05
	$^{13}C_6$	**$^{13}C_7$**	**$^{13}C_8$**	**$^{13}C_9$**	**^{18}O**
A/MHz	1922.22159(18)	1902.37298(48)	1899.23767(29)	1919.00840(40)	1895.75670(29)
B/MHz	1293.52330(14)	1290.13956(13)	1286.92061(10)	1277.10613(11)	1266.94249(39)
C/MHz	1160.63618(10)	1161.766614(98)	1159.804706(77)	1146.468358(82)	1130.08034(32)
Δ_J/kHz	0.1016(15)	0.10113(91)	0.10215(98)	0.09883(79)	0.1035(35)
Δ_{JK}/kHz	-0.0973(84)	-0.0853(62)	-0.0882(58)	-0.0796(60)	-
Δ_K/kHz	-	0.094(35)	0081(23)	0.151(28)	-
δ_J/kHz	0.0296(10)	0.02897(90)	0.03010(82)	0.02842(79)	0.0297(32)
N	38	35	32	32	21
RMS/kHz	1.13	0.67	0.59	0.57	2.2

of the experimental to the calculated corresponding rotational constants of the parent species, making the search for the lines very fast. The fitted rotational and centrifugal distortion constants for all isotopologues in natural abundance are assembled in Table 2. If not fitted, the values of the centrifugal distortion parameters were kept fixed to the corresponding values of the parent molecule (Table 1).

As recently reported in the high-resolution spectroscopic study of camphene,[21] a few rotational lines of β-pinene and nopinone also display complex line-shapes with several components of various intensities separated by a few tens of kHz. Each complex line-shape is associated with the magnetic interaction between close nuclear hydrogen spins. Interestingly it was shown that the hyperfine structure could be well modelled by only considering the pairs of hydrogen atoms from the three $(-CH_2-)$ methylene groups without consideration for the $(=CH_2)$ group contribution. As in camphene the hyperfine geometrical parameters were evaluated using the MP2/aug-cc-pVTZ structure. Indeed for two nuclear spins denoted $\boldsymbol{I_1}$ and $\boldsymbol{I_2}$, the nuclear spin-spin Hamiltonian can be written as:[45-46]

$$H_{ss} = \boldsymbol{I_1}.\boldsymbol{D}.\boldsymbol{I_2}$$

in which the second-rank direct dipolar spin-spin coupling tensor $\boldsymbol{D}$ contains information about the inter-nuclear vectors. The tensor elements are defined by

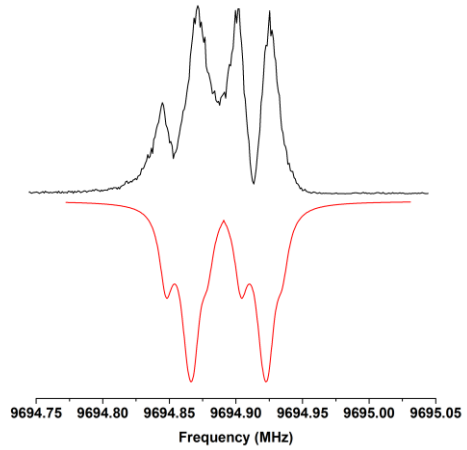

Figure 3 Experimental (black) and simulated (red) hyperfine structure associated with the $J_{KaKc} = 3_{21} - 2_{12}$ line of β-pinene. Lorentzian line shapes with a full width at half maximum equal to 11 kHz were adjusted to each hyperfine component.

$$D_{ij}^{12} = g_1 g_2 \frac{\mu_0 \mu_N^2}{4\pi} \frac{R^2 \delta_{ij} - 3\boldsymbol{R_i R_j}}{R^5}$$

g_1 and g_2 are the nuclear g factors for nuclei 1 and 2, μ_N is the nuclear magneton, $\boldsymbol{R_i}$ and $\boldsymbol{R_j}$ are the position vectors of nuclei in the principal inertial axis system, with $i, j = a, b, c$ and R is the length of the vector joining the two nuclei. The associated line shapes were simulated using the SPCAT program[42], with a Lorentz profile adjusted on each calculated hyperfine component. As illustrated in Figure 3 for β-pinene, a good agreement is observed on the frequency scale, while it is more qualitative on the intensity scale, because of a cavity mode residue.

Molecular structures

All the results presented in this section have been obtained by using the computer programs STRFIT and KRA.[47] Experimental rotational parameters have been obtained for the parent molecules and for substituted ^{13}C and ^{18}O isotopologues. Consequently it became possible to determine the substitution structure (r_s) for the heavy atoms skeleton. At first the coordinates were calculated using Kraitchman's equations,[27] with the uncertainties from vibration-rotation effects as estimated by Costain.[28] It has been pointed out that for very small coordinates, the r_s method may lead to a square root of a negative number, that is, an imaginary coordinate.[48] This is the case with one c_s imaginary coordinate for the atom C_5 and one another a_s imaginary coordinate for the atom C_1, for both molecules (see supplementary materials). Therefore it was not possible to find all the geometrical parameters from the r_s structure. As recommended in the literature[48] we evaluated two other geometries in order to determine the molecular structure of heavy atoms: the ground state effective geometry (r_0) and the equilibrium related mass-dependence geometry ($r_m^{(1)}$).[29-30] There are 33 experimental moments of inertia, the geometry of the heavy atom skeleton consisting of 10 atoms will be completely determined by 3N - 6 = 24 internal coordinates. Because only heavy atom substitution was investigated by fitting the molecular geometry directly to all observed moments of inertia, these two geometries require several subsidiary assumptions. To this end all CH bond lengths and CCH angles were taken from the *ab initio* MP2 calculations. The best results are presented in Tables 3 and 4, *i. e.* using the MP2/6-311++G(d,p) and MP2/aug-cc-pVTZ equilibrium geometries for the r_0 and $r_m^{(1)}$ structures, respectively. Only a subset of these parameters, 9 distances and 8 angles constituted the actual parameters of fit. The other tabulated parameters were derived from statistically identical fits involving modified declarations of molecular geometry. In the $r_m^{(1)}$ structures the vibration-rotation contributions are obtained through the c_α coefficients. It should be noted that both r_0 and $r_m^{(1)}$ skeleton geometries of β-pinene and nopinone were obtained without any structural assumption.

Discussion

β-pinene structure

The least-squares of both r_0 and $r_m^{(1)}$ skeleton geometries show a good precision of determination for all structural parameters. The best residual of the fit is obtained for the $r_m^{(1)}$ structure (0.0075 uÅ²), and the same result is obtained using the MP2/6-311++G(d,p) or the MP2/aug-cc-pVTZ equilibrium geometries. A slightly better standard deviation was obtained for the r_0 geometry with the MP2/6-311++G(d,p) structure (0.0080 uÅ²) than with the MP2/aug-cc-pVTZ structure (0.0087 uÅ²), probably because of the better reproduction of the rotational constants for the parent molecule.

The gas-phase structure of β-pinene can be compared with parameters obtained by X-ray crystallography.[18] A big difference is observed in the C_2, C_3, C_4, and C_{10} structure. This is due to the force in the crystal structure exerted in this part of the molecule. In particular the dihedral angles $C_2C_3C_4C_5$, $C_6C_1C_2C_{10}$ and $C_{10}C_2C_3C_4$ are affected, when compared to the gas phase structure. Also this difference between the two gas and crystal phases is observed especially in the C_2C_{10} and C_4C_5 bond lengths, *i.e.* they are much shorter in the crystal phase than in the gas phase.

The structure of β-pinene is also compared with the available data on bicyclo[3.1.1]heptane[49] which has the similar bicyclic structure. The comparison is based on the $r_m^{(1)}$ structures. The bond lengths are very close but some angles differ significantly. In particular the $C_1C_2C_3$ angle value is smaller by 5.5° in bicyclo[3.1.1]heptane. This can be explained by the double bond between the methylene group and the C_2 atom. The two angles values of $C_7C_1C_6$ and $C_7C_5C_6$ are also smaller by 1.7° and 1.9° in the case of bicyclo[3.1.1]heptane. On one hand this is due to the attachment of the two methyl groups to the C_6 atom. In the other hand this attachment of the methyl groups also can explain that the angle values of $C_7C_5C_4$ and $C_7C_1C_2$ are greater in the case of bicyclo[3.1.1]heptane.

Table 3 Comparison of the geometrical parameters (lengths/Å and angles/°) values determined experimentally and theoretically for the heavy atoms of β-pinene, and with those of related species.

		β-pinene			Bicyclo[3.1.1] heptane	Camphene	Norbornane
	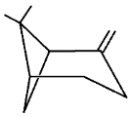				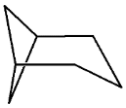	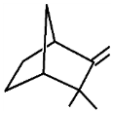	
Parameter	r_0	$r_m^{(1)}$	X-Ray[a]	MP2-AVTZ	Elec. diffraction[b]	$r_m^{(1)}$[c]	Elec. diffraction[d]
$r(C_3C_2)$	1.525(8)	1.513(10)	1.519(3)	1.513	1.534(30)	–	–
$r(C_4C_3)$	1.548(6)	1.546(7)	1.547(3)	1.545	1.534(30)	–	–
$r(C_4C_5)$	1.541(8)	1.530(12)	1.517(3)	1.527	1.511(15)	–	–
$r(C_5C_6)$	1.556(9)	1.546(10)	1.543(3)	1.558	1.553(9)	1.545(4)	1.536(15)
$r(C_1C_6)$	1.578(10)	1.561(15)	1.562(3)	1.569	1.553(9)	1.519(3)	1.573(15)
$r(C_1C_{10})$	1.340(5)	1.339(5)	1.320(3)	1.339	–	1.343(5)	–
$r(C_7C_5)$	1.556(12)	1.563(13)	1.543(3)	1.549	1.553(9)	1.546(4)	1.546(24)
$r(C_6C_8)$	1.524(12)	1.538(16)	1.521(3)	1.517	–	1.535(8)	–
$r(C_6C_9)$	1.537(7)	1.526(9)	1.523(3)	1.523	–	1.544(7)	–
$r(C_1C_2)$	1.495(11)	1.491(13)	1.500(3)	1.494	1.511(15)	–	–
$r(C_1C_7)$	1.562(6)	1.556(8)	1.547(3)	1.553	1.553(9)	1.540(4)	1.546(24)
$\angle(C_2C_3C_4)$	113.4(2)	113.4(2)	114.1(2)	113.0	113.0(18)	–	–
$\angle(C_5C_4C_3)$	111.3(3)	111.5(4)	112.4(2)	110.8	108.7(11)	–	–
$\angle(C_4C_5C_6)$	110.8(6)	111.9(9)	111.1(1)	110.6	–	–	–
$\angle(C_1C_6C_5)$	85.7(5)	86.6(8)	85.3(1)	85.6	87.1(10)	94.1(2)	93.41(9)
$\angle(C_{10}C_2C_3)$	122.5(5)	123.2(6)	122.5(2)	123.0	–	126.8(4)	–
$\angle(C_7C_5C_4)$	108.9(5)	108.5(5)	109.2(2)	109.3	110.9(6)	–	–
$\angle(C_8C_6C_5)$	119.6(8)	118.1 (11)	118.8(2)	119.1	–	114.1(4)	–
$\angle(C_9C_6C_1)$	111.3(10)	112.9(12)	112.4(1)	111.6	–	111.5(6)	–
$\angle(C_{10}C_2C_1)$	123.3(6)	123.2(6)	122.8(2)	123.0	–	125.8(4)	–
$\angle(C_8C_6C_9)$	108.7(6)	107.9(7)	108.9(2)	109.1	–	–	–
$\angle(C_8C_6C_1)$	118.0(5)	117.7(6)	117.9(2)	118.0	–	113.0(10)	–
$\angle(C_9C_6C_5)$	112.0(6)	112.8(7)	112.0(1)	111.8	–	109.7(6)	–
$\angle(C_5C_7C_1)$	86.3(4)	86.1(3)	86.5(2)	86.4	87.1(10)	–	–
$\angle(C_7C_5C_6)$	88.1(6)	86.8(8)	87.7(2)	87.7	84.9(14)	–	–
$\angle(C_2C_1C_7)$	109.3(6)	109.7(7)	108.7(2)	109.3	110.9(6)	–	–
$\angle(C_1C_2C_3)$	114.2(4)	114.2(4)	114.6(1)	114.0	108.7(11)	–	–
$\angle(C_2C_1C_6)$	108.9(6)	109.5(7)	110.1(1)	108.2	–	–	–
$\angle(C_7C_1C_6)$	87.0(5)	86.6(7)	87.5(2)	87.2	84.9(14)	–	–
$\angle(C_2C_3C_4C_5)$	-21.6(9)	-21.5(9)	-13.3(3)	-24.6	–	–	–
$\angle(C_3C_4C_5C_6)$	58.6(9)	57.1(13)	54.7(3)	60.1	–	–	–
$\angle(C_4C_5C_6C_1)$	-82.7(8)	-81.0(15)	-82.9(2)	-83.1	–	–	–
$\angle(C_6C_1C_2C_{10})$	118.8(12)	119.2(11)	126.1(2)	116.9	–	–	–
$\angle(C_3C_4C_5C_7)$	-36.6(5)	-37.0(5)	-40.4(3)	-34.9	–	–	–
$\angle(C_2C_1C_6C_8)$	-38.6(9)	-38.1(9)	-37.9(3)	-37.9	–	–	–
$\angle(C_2C_1C_6C_9)$	-165.3(6)	-164.8(7)	-165.7(2)	-165.4	–	–	–
$\angle(C_4C_5C_6C_8)$	37.2(7)	38.7(10)	36.4(3)	36.6	–	–	–
$\angle(C_7C_1C_6C_5)$	-26.6(5)	-27.8(8)	-26.7(2)	-26.7	–	–	–
$\angle(C_{10}C_2C_3C_4)$	-155.8(8)	-156.0(8)	-167.5(2)	-152.7	–	–	–
$\angle(C_{10}C_2C_3C_1)$	-179.5(5)	-180.3(16)	-181.4	-179.6	–	–	–
σ_{fit}/(uÅ^2)	0.0080	0.0075[e]	–	–	–	–	–

[a] Ref. 18 ; [b] Ref. 49 ; [c] Ref. 21 ; [d] Ref. 50 ; [e] $c_a = 0.137(63)$ u$^{1/2}$ Å, $c_b = 0.092(56)$ u$^{1/2}$ Å, $c_c = 0.082(58)$ u$^{1/2}$ Å.

Finally a few structural parameters of β-pinene have been compared with two bicyclic molecules: camphene[21] and norbornane.[50] The bond lengths values are very close except the C_1C_6 value which is smaller in the case of camphene. This may be due to the proximity of the double bond and of the methyl groups in the case of camphene. It is also remarkable that the angle involving the bridged carbon C_7 is quite greater in the case of camphene and norbornane than in β-pinene while the other angle values differ slightly between the camphene and the β-pinene. Concerning the $(= CH_2)$ group, the value obtained for the $C = C$ bond length in β-pinene and camphene are very similar, and the value of the $C_{10}C_2C_3C_1$

dihedral angle confirm the planarity of this sub-structure in the gas phase.

Table 4 Comparison of the geometrical parameters (lengths/Å and angles/°) values determined experimentally and theoretically for the heavy atoms of nopinone, and with those of related species.

		Nopinone			Camphor	Fenchone
		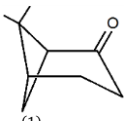			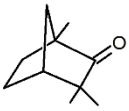	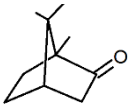
Parameter	r_0	$r_m^{(1)}$	$\Delta\, r_m^{(1)}$ [a]	MP2-AVTZ	$r_m^{(1)}$ [b]	r_0 [c]
$r(C_3C_2)$	1.535(7)	1.525(10)	0.012	1.529	1.528(3)	1.535(31)
$r(C_4C_3)$	1.546(6)	1.544(8)	-0.002	1.549	–	–
$r(C_4C_5)$	1.542(7)	1.533(13)	0.003	1.530	–	–
$r(C_5C_6)$	1.553(9)	1.545(11)	-0.001	1.560	1.548(8)	1.552(8)
$r(C_2C_1)$	1.501(11)	1.499(13)	0.008	1.500	1.538(7)	1.526(29)
$r(C_7C_5)$	1.551(10)	1.559(13)	-0.004	1.551	–	–
$r(C_8C_6)$	1.528(12)	1.539(18)	0.001	1.525	1.544(4)	–
$r(C_9C_6)$	1.535(7)	1.526(10)	0.000	1.529	1.532(3)	–
$r(OC_2)$	1.214(4)	1.215(5)	–	1.220	1.213(1)	1.214(5)
$r(C_7C_1)$	1.561(6)	1.554(8)	-0.002	1.550	–	–
$r(C_1C_6)$	1.579(11)	1.564(18)	0.003	1.570	1.524(7)	1.541(25)
$\angle(C_2C_3C_4)$	114.1(2)	114.1(2)	0.7	113.9	–	–
$\angle(C_5C_4C_3)$	111.3(3)	111.5(4)	0.0	111.1	–	–
$\angle(C_6C_5C_4)$	111.1(5)	111.9(10)	0.0	110.9	102.7(2)	–
$\angle(C_1C_2C_3)$	114.9(4)	115.0(4)	0.8	114.4	–	–
$\angle(C_7C_5C_4)$	108.7(5)	108.4(6)	-0.1	109.1	–	–
$\angle(C_8C_6C_1)$	117.6(5)	117.5(6)	-0.2	117.9	113.1(3)	–
$\angle(C_9C_6C_5)$	112.1(6)	112.7(9)	-0.1	111.9	113.9(3)	–
$\angle(C_7C_5C_6)$	88.3(5)	87.5(9)	-0.7	87.9	–	–
$\angle(C_5C_6C_1)$	85.9(6)	86.6(8)	0.0	85.9	94.6(2)	95.2(6)
$\angle(C_6C_1C_7)$	87.1(5)	86.9(7)	0.3	87.3	–	–
$\angle(C_6C_1C_2)$	107.7(6)	108.2(3)	-1.2	106.6	100.7(3)	–
$\angle(OC_2C_3)$	121.4(6)	121.3(6)	–	122.2	127.0(1)[d]	125.8(31)
$\angle(OC_2C_1)$	123.6(6)	123.7(7)	–	123.4	127.0(1) [d]	–
$\angle(C_2C_1C_7)$	108.7(5)	108.8(8)	-0.9	109.4	–	–
$\angle(C_8C_6C_5)$	119.9(8)	118.8(12)	0.7	119.2	113.7(3)	–
$\angle(C_9C_6C_1)$	111.0(8)	112.1(13)	-0.8	111.1	114.0(5)	–
$\angle(C_5C_7C_1)$	86.7(6)	86.5(4)	0.4	86.9	–	–
$\angle(C_8C_6C_9)$	108.7(6)	108.0(8)	0.1	109.2	107.3(2)	–
$\angle(C_5C_4C_3C_2)$	-16.1(9)	-15.8 (10)	5.7	-19.2	–	–
$\angle(C_6C_5C_4C_3)$	55.5(8)	54.4(15)	-2.7	56.4	–	–
$\angle(C_1C_2C_3C_4)$	18.8(11)	18.9(12)	-5.4	22.9	–	–
$\angle(C_7C_5C_4C_3)$	-40.1(5)	-40.4(6)	-3.4	-38.9	–	–
$\angle(C_8C_6C_1C_2)$	-38.7(8)	-38.4(10)	-0.3	-37.2	–	–
$\angle(C_9C_6C_5C_4)$	165.3(8)	164.9(10)	-0.6	165.0	–	–
$\angle(OC_2C_1C_7)$	-145.7(11)	-145.8(12)	–	-148.6	–	–
$\angle(OC_2C_1C_6)$	121.3(9)	121.2(10)	–	118.3	–	–
$\angle(OC_2C_3C_4)$	-160.7(9)	-160.5(9)	–	-156.7	–	–
$\angle(C_8C_6C_5C_4)$	36.0(7)	37.1(11)	-1.5	35.9	–	–
$\angle(C_8C_6C_5C_7)$	145.4(5)	145.9(7)	0.5	145.6	–	–
$\angle(C_9C_6C_5C_7)$	-85.3(8)	-86.2(12)	-0.4	-85.4	–	–
$\angle(C_4C_5C_7C_1)$	85.7(5)	85.8(7)	1.5	85.4	–	–
$\angle(C_4C_5C_6C_1)$	-83.8(7)	-82.3(11)	-1.3	-83.9	–	–
$\angle(OC_2C_3C_1)$	-179.5(14)	-179.6(16)	–	-179.5		
σ_{fit}/(uÅ^2)	0.0079	0.0082[e]	–	–	0.0040	–

[a] Difference with the corresponding value for β-pinene ; [b] Ref. 22 ; [c] Ref. 23 ;[d] $\angle(OC_2C_3) = \angle(OC_2C_1)$ and a planar centre at C_2 assumed ; [e] $c_a = 0.115(68)$ u$^{1/2}$ Å, $c_b = 0.076(58)$ u$^{1/2}$ Å, $c_c = 0.0073(59)$ u$^{1/2}$ Å.

Journal Name

ARTICLE

Nopinone structure

As seen in Table 4, a slightly better standard deviation was obtained for the r_0 geometry of nopinone with the MP2/6-311++G(d,p) structure (0.0079 uÅ²) than with the MP2/aug-cc-pVTZ structure (0.0085 uÅ²), again probably because of the better reproduction of the rotational constants for the parent molecule. Meanwhile a slightly better standard deviation was obtained for the $r_m^{(1)}$ structure using the MP2/aug-cc-pVTZ structure (0.0082 uÅ²) than with the MP2/6-311++G(d,p) one (0.0083 uÅ²).

The present gas-phase structure of nopinone cannot be compared with the crystal structure of the low-temperature phase of the molecule.[19] Indeed all bond distances and angles were constrained to the values derived from a molecular orbital optimisation of the molecular structure using a 6-31G(d') basis set.

Meanwhile the structure of nopinone can be compared with the available data for two bicyclic ketone molecules: camphor and fenchone. The bond length are very close except the C_1C_2 bond value which is smaller in the case of nopinone. This may be due to the small ring of four atoms present in the case of nopinone. Also the small bridge angle of C_7 is forcing the bond length of C_1C_2 to be smaller. It is also remarkable that the two angles with carbonyl groups OC_2C_1 and OC_2C_3 are smaller in nopinone while the $C_2C_1C_6$ and $C_4C_5C_6$ angles are bigger. The other effect associated with the four atoms ring is that the bridge involved the C_4 atom is forced to be far from the five atoms ring. It is remarkable that the angles $C_5C_6C_8$ and $C_1C_6C_8$ are respectively bigger and smaller in nopinone than in camphor. Concerning the ketone group, the value obtained for the $C = O$ bond length in nopinone, camphor and fenchone are very similar. The value of the $OC_2C_3C_1$ dihedral angle confirms the planarity of this sub-structure in the gas phase.

Structural effects of the oxidation process

The $r_m^{(1)}$ structures of the reagent β-pinene and of its oxidation product nopinone have been compared in Table 4. It is clear that the two molecules have a similar skeleton structure except for their respective functional groups. Meanwhile a few striking features can be pointed out. Clearly the C_2C_3 bond length is shorter in β-pinene than in nopinone. The same situation was observed in the case of camphene and fenchone, and recognized as a signature of the C_2 substituent.[23] A second change between the two structures is the dihedral angle values $C_2C_3C_4C_5$ and $C_1C_2C_3C_4$ which are respectively 5.7° bigger and 5.4° lower in nopinone than in β-pinene. This can be explained by the fact that C_2 being a centre of planarity in both molecules (value of the dihedral angles $C_{10}C_2C_3C_1$ and $OC_2C_1C_3$) in the gas phase, the variation of the C_2C_3 bond length is compensated by the dihedral angles values.

Finally we should mention the recent study on two bicyclic ethers, eucalyptol and 1,4-cineole, by broadband rotational spectroscopy.[51] It is of particular relevance as it compares structures of bicyclic ethers with atmospheric importance. In particular the authors pointing out i) the relatively unstrained structure of eucalyptol compared to 1,4-cineole and ii) the relative higher atmospheric reactivity of eucalyptol as being not due to the straining or weakening of bonds within the bicyclic structure.

Conclusions

We have observed for the first time the rotational spectra of β-pinene and nopinone. The rotational constants of the parent, and all ^{13}C and ^{18}O isotopologues in natural abondances, have been determined with accuracy for the ground state. Theoretical calculations with density functional and *ab initio* methods have been performed to obtain the equilibrium structure. Combining experimental and theoretical data, the gas-phase structures of β-pinene and nopinone have been determined for the first time. Indeed the ground-state (r_0) and the equilibrium related, mass-dependence ($r_m^{(1)}$) geometries of the skeletons have been obtained with no structural assumption, but using the theoretically calculated CH bond lengths and CCH angles. The best fits were obtained using the *ab initio* values of these parameters. In particular we have experimentally observed that C_2 is a centre of planarity in both molecules. The gas-phase structure of β-pinene was compared to the crystal phases, the latest showing a defect to planarity for the C_2 centre. The $r_m^{(1)}$ structures of β-pinene and nopinone were found remarkably similar. The oxidation process of β-pinene is leading to the formation of nopinone with only three structural changes, associated with the variation of the bond length between C_2 and the adjacent methylene group, and the variation of the associated dihedral angles. These structural changes are obviously conducted by the substituent at C_2. The full experimental determination of the skeleton structures of two bicyclic monoterpenes of atmospheric interest in the gas phase, should pave the way for the characterization of oxidation processes.

To highlight the physical importance of the present data we can stress the importance of quantum chemical calculations used to model monoterpenes kinetics. Quantum chemistry calculations are suitable for establishing reaction mechanisms and have been widely employed for the description of the

ozone initiated atmospheric reactions of unsaturated compounds including monoterpenes. The computational procedures include geometry optimizations. It is not so easy to optimize a structure of monoterpenes at a reasonable cost. Therefore we believe that our results could be used by theoreticians as a test case.

Acknowledgements

Dr. N. Savoia is gratefully acknowledged for recording high-resolution lines of β-pinene. The present work was funded by the French ANR *Labex CaPPA* through the PIA under contract ANR-11-LABX-0005-01, by the Regional Council *Hauts-de-France*, by the European Funds for Regional Economic Development (FEDER), and by the contract CPER CLIMIBIO.

Notes and references

1 M. Ehn, J. A. Thornton, E. Kleist, et al., *Nature*, 2014, **506**, 476.
2 Y. S. Son, K. J. Kim, I. H. Jung, S. J. Lee, and J. C. Kim., *J. Atmos. Chem.,* 2015, **72(1)**, 27.
3 S. Owen, C. Boissard, R. A. Street, S. C. Duckham, O. Csiky, and C.N. Hewitt, *Atmos. Env.*, 1997, **31**, 101.
4 J. Kesselmeier, U. Kuhn, A. Wolf, M.O. Andreae, P. Ciccioli, E. Brancaleoni, M. Frattoni, A. Guenther, J. Greenberg, P. De Castro Vasconcellos, T. de Oliva, T. Tavares, and P. Artaxo. *Atmos. Env.*, 2000, **34(24)**, 4063**.**
5 R. Atkinson and J. Arey, *Acc. Chem. Res.*, 1998, **31(9)**, 574.
6 R. Atkinson and J. Arey, *Atmos. Env.*, 2003, **37**, 197.
7 S. S. Brown, W. P. Dubé, R. Bahreini, A. M. Middlebrook, C. A. Brock, C. Warneke, J. A. De Gouw, R. A. Washenfelder, E. Atlas, J. Peischl, et al., *Atmos. Chem. Phys.*, 2013, **13(22)**, 11317.
8 R. J. Griffin, D. R. Cocker III, J. H. Seinfeld, and D. Dabdub, *Geophys. Res. Lett.*, 1999, **26(17)**, 2721.
9 J. Yu, D. R. Cocker III, R. J. Griffin, R. C. Flagan, and J. H. Seinfeld, *J. Atmos. Chem.*, 1999, **34(2)**, 207.
10 R. Winterhalter, P. Neeb, D. Grossmann, A. Kolloff, O. Horie and G. Moortgat, *J. Atmos. Chem.*, 2000, **35**, 165.
11 D. Zhang and R. Zhang, *J. Chem. Phys.*, 2005, 122, 114308.
12 A. Calogirou, B. R. Larsen, and D. Kotzias, *Atmos. Env.*, 1999, **33**, 1352.
13 R. Larsen, D. Di Bella, M. Glasius, R. Winterhalter, N. R. Jensen and J. Hjorth, *J. Atmos. Chem.*, 2001, **38**, 231.
14 S. S. Brown, W. P. Dubé, R. Bahreini, A. M. Middlebrook, C. A. Brock, C. Warneke, J. A. de Gouw, R. A. Washenfelder, E. Atlas, J. Peischl, T. B. Ryerson, J. S. Holloway, J. P. Schwarz, R. Spackman, M. Trainer, D. D. Parrish, F. C. Fehshenfeld, and A. R. Ravishankara, *Atmos. Chem. Phys.*, 2013, **13**, 11317.
15 R. J. Griffin, D. R. Cocker, and J. H. Seinfeld, *Geophys. Res. Lett.*, 1999, **26(17)**, 2721.
16 T. L. Nguyen, J. Peeters and L. Vereecken, *Phys. Chem. Chem. Phys.*, 2009, **11**, 5643.
17 R. C. de M. Oliveira and G. F. Bauerfeldt, *J. Phys. Chem. A*, 2015, **119**, 2802.
18 A. D. Bond and J. E. Davies, *Acta Crystallogr. Sect. E*, 2001, **E57**, 1041.
19 L. Palin, M. Brunelli, J. P. Wright, P. Pattison and A. N. Fitch, *Z. Kristallogr.*, 2008, **223**, 602.
20 J. R. Aviles Moreno, T. R. Huet, J. J. Lopez Gonzalez, *Struct. Chem.*, 2013, **24**, 1163.
21 E. M. Neeman, P. Dréan and T. R. Huet, *J. Mol. Spectrosc.*, 2016, **322**, 50.
22 Z. Kisiel, O. Desyatnyk, E. Bialkowska-Jaworska and L. Pszczólkowski, *Phys. Chem. Chem. Phys.*, 2003, **5**, 820.
23 D. Loru, M. A. Bermúdez, and M. E. Sanz, *J. Chem. Phys.*, 2016, 145, 074311.
24 T. J. Balle and W. H. Flygare, *Rev. Sci. Instrum.*, 1981, **52(1)**, 33.
25 J.-U. Grabow, W. Stahl, H. Dreizler, *Rev. Sci. Instrum.*, 1996, **67(12)**, 4072.
26 J.-U. Grabow, in *Handbook of high-resolution spectroscopy*, Vol 2, M. Quack and F. Merkt Ed., Wiley 2011.
27 J. Kraitchman, *Am. J. Phys.*, 1953, **21**, 17.
28 C. C. Constain, *Trans. Am. Crystallogr. Assoc.*, 1966, **2**, 157.
29 J. K. G. Watson, *J. Mol. Spectrosc.*, 1973, **48(3)**, 479.
30 J. K. G. Watson, A. Roytburg, W. Ulrich, *J. Mol. Spectrosc.*, 1999, **196**, 102.
31 S. Kassi, PhD thesis, University of Lille (2000).
32 M. Tudorie, L. H. Coudert, T. R. Huet, D. Jegouso and G. Sedes, *J. Chem. Phys.*, 2011, **134**, 074314.
33 Gaussian 09, Revision D.01, M. J. Frisch, G. W. Trucks, H. B. Schlegel, G. E. Scuseria, M. A. Robb, J. R. Cheeseman, G. Scalmani, V. Barone, B. Mennucci, G. A. Petersson, H. Nakatsuji, M. Caricato, X. Li, H. P. Hratchian, A. F. Izmaylov, J. Bloino, G. Zheng, J. L. Sonnenberg, M. Hada, M. Ehara, K. Toyota, R. Fukuda, J. Hasegawa, M. Ishida, T. Nakajima, Y. Honda, O. Kitao, H. Nakai, T. Vreven, J. A. Montgomery, Jr., J. E. Peralta, F. Ogliaro, M. Bearpark, J. J. Heyd, E. Brothers, K. N. Kudin, V. N. Staroverov, T. Keith, R. Kobayashi, J. Normand, K. Raghavachari, A. Rendell, J. C. Burant, S. S. Iyengar, J. Tomasi, M. Cossi, N. Rega, J. M. Millam, M. Klene, J. E. Knox, J. B. Cross, V. Bakken, C. Adamo, J. Jaramillo, R. Gomperts, R. E. Stratmann, O. Yazyev, A. J. Austin, R. Cammi, C. Pomelli, J. W. Ochterski, R. L. Martin, K. Morokuma, V. G. Zakrzewski, G. A. Voth, P. Salvador, J. J. Dannenberg, S. Dapprich, A. D. Daniels, O. Farkas, J. B. Foresman, J. V. Ortiz, J. Cioslowski, and D. J. Fox, Gaussian, Inc., Wallingford CT, 2013.
34 http://www.chemcraftprog.com.
35 C. Møller, M. S. Plesset, *Phys. Rev.*, 1934, **46**, 618.
36 T. H. J. Dunning, *J. Chem. Phys.*, 1989, **90**, 1007.
37 L. A. Curtiss, K. Raghavachari, P. C. Redfern, V. Rassolov, J. A. Pople, *J. Chem. Phys.*, 1998, **109**, 7764.
38 A. D. Becke, *J. Chem. Phys.*, 1993, **98**, 5648.
39 C. Lee, W. Yang, R.G. Parr, *Phys. Rev. B*, 1988, **37**, 785.
40 Y. Zhao, D. G. Truhlar, *Theor. Chem. Acc.*, 2008, **120**, 215.
41 Y. Zhao, D. G. Truhlar, *Acc. Chem. Res.*, 2008, **41(2)**, 157.
42 J. K. G. Watson, in Vibrational Spectra and Structure, *J. R. Durig, Ed., Elsevier, Amsterdam,* 1977**, 6,** 1.
43 H. M. Pickett, J. Mol. Spectrosc., 1991, **148**, 371.
44 Z. Kisiel, in J. Demaison et al (Eds.), *Spectroscopy from Space*, Kluwer Academic Publishers, Dordrecht (2001) 91-106 ; PROSPE – Programs for ROtational SPEctroscopy, Institute of Physics, Academy of Science, Warsaw, http:// www.ifpan.edu.pl/~kisiel/prospe.htm.
45 P. Thaddeus, L.C. Krisher, J.H.N. Loubster, *J. Chem. Phys.*, 1964, **40**, 257.
46 A. Carrington, J. M. Brown, *Rotational Spectroscopy of Diatomic Molecules*, Cambridge University Press, Cambridge, 2003**.**
47 Z. Kisiel, *J. Mol. Spectrosc.*, 2003, **218**, 58.
48 H. D. Rudolph and J. Demaison, in *Equilibrium Molecular Structures: From Spectroscopy to Quantum Chemistry*, J. Demaison, J.E. Boggs and A.G. Császár, Ed., CRC Press 2010, p. 125-158.
49 G. Dallinga and L. H. Toneman, Recueil des Travaux Chimiques des Pays-Bas, 1969, **88(2**), 185.
50 L. Doms, L. Van den Enden, H. J. Geise, and C. Van Alsenoy, *J. Am. Chem. Soc.*, 1983, **105**, 158.
51 C. Medcraft and M. Schnell, Z. Phys. Chem. 2016, **130(1)**, 1.